

***Ab initio* thermodynamics of the hcp metals Mg, Ti, and Zr**Yaozhuang Nie<sup>1,2</sup> and Youqing Xie<sup>2</sup><sup>1</sup>*School of Physics Science and Technology, Central South University, Changsha, 410083 China*<sup>2</sup>*School of Material Science and Engineering, Central South University, Changsha, 410083 China*

(Received 5 November 2006; revised manuscript received 7 February 2007; published 29 May 2007)

The thermal properties of hcp metals Mg, Ti, and Zr are investigated by performing density functional theory and density functional perturbation theory calculations within the quasiharmonic approximation. The temperature dependence of various quantities such as the anisotropic thermal expansion, the heat capacity, bulk modulus, and Grüneisen parameters are computed. The electronic contribution to the thermal expansion and heat capacity are discussed. Our results are in good agreement with available experimental data in a wide range of temperature.

DOI: [10.1103/PhysRevB.75.174117](https://doi.org/10.1103/PhysRevB.75.174117)

PACS number(s): 65.40.De, 65.40.Ba, 71.15.Dx, 71.15.Mb

**I. INTRODUCTION**

Nowadays the equilibrium structure of a large class of materials can be determined within first-principles methods based on density functional theory (DFT).<sup>1–3</sup> Furthermore, different approaches have been used to calculate thermal properties from first-principles.<sup>4</sup> Thermal properties of solids such as thermal expansion depend on their lattice dynamical behavior. A simplified method for thermal expansion calculations is a Debye–Grüneisen based model.<sup>5</sup> Thermal expansion calculations for metals<sup>6,7</sup> and compounds<sup>8</sup> have been carried out based on this model. A more accurate approach is first-principles molecular dynamics (MD) simulations such as Car–Parrinello method.<sup>9</sup> However, since the ionic degrees of freedom are treated classically, these simulations are not valid at temperatures comparable to or lower than the Debye temperature. In the 1990's, another approach had been made possible by the achievements of density functional perturbation theory (DFPT)<sup>10,11</sup> which allowed exact calculations of vibrational frequencies in every point of the Brillouin Zone. Since then, many applications have been made within DFPT.<sup>4</sup> The vibrational free energy can be obtained using the quasiharmonic approximation. In this approximation, anharmonic effects are included through the explicit volume dependence of the vibrational frequencies. Several thermal expansion calculations about cubic metals based on DFPT have been carried out,<sup>12–15</sup> and they give good results about isotropic thermal expansion and related thermal properties. For noncubic structure, because of the large computational cost of determining the complete phonon spectrum as a function of volume, few thermal expansion calculations based on DFPT have been carried out.<sup>16</sup> In this paper we apply DFPT within quasiharmonic approximation to the study of the anisotropic thermal expansion for hcp metals Mg, Ti, and Zr. Another purpose of the present paper is to check the electronic contribution to the thermal properties which previous calculations often neglected. As a by-product, bulk modulus and heat capacities at constant volume (pressure) are also calculated. Our results demonstrate that all these quantities can be well predicted by this approach in a wide range of temperature.

**II. THEORY**

The equilibrium structural parameters,  $\mathbf{a}=(a_1, a_2, \dots)$ , of a crystal at any temperature,  $T$ , are obtained by minimizing

the Helmholtz free energy,  $F$ , of a system. The free energy  $F$  at temperature  $T$  and structural parameters  $\mathbf{a}$  is given by

$$F(\mathbf{a}, T) = E_{\text{tot}}(\mathbf{a}) + k_B T \sum_{q\lambda} \ln \left[ 2 \sinh \left( \frac{\hbar \omega_{q\lambda}(\mathbf{a})}{2k_B T} \right) \right] + E_{\text{el}}(\mathbf{a}, T) - TS_{\text{el}}(\mathbf{a}, T) \quad (1)$$

where  $E_{\text{tot}}(\mathbf{a})$  is the ground state ( $T=0$  K) total energy of the crystal. The next term is the vibrational free energy. The electronic energy due to thermal electronic excitations is given by

$$E_{\text{el}}(V, T) = N \int_0^\infty n(\varepsilon, V) f(\varepsilon) \varepsilon d\varepsilon - N \int_0^{\varepsilon_F} n(\varepsilon, V) \varepsilon d\varepsilon, \quad (2)$$

where  $n(\varepsilon, V)$  and  $f(\varepsilon)$  represent the electronic density of state (DOS) and the Fermi–Dirac (FD) distribution, respectively. The electronic entropy is formulated as

$$S_{\text{el}}(V, T) = -Nk_B \int_0^\infty n(\varepsilon, V) [f \ln f + (1-f) \ln(1-f)] d\varepsilon. \quad (3)$$

It is often assumed that the electronic contribution to free energy is negligible.

To calculate free energy  $F$ , one must be able to calculate frequencies all over the Brillouin zone, and this can be done exactly using DFPT. Furthermore, this calculation must be performed at various values of the structural parameters. Because of this, it is difficult from a computational point of view. In the case of anisotropic thermal expansion of an hcp crystal, the system is described by two parameters,  $a$  and  $c$ . One can compute phonon dispersions in a grid of points in the  $(a, c)$  space and obtain phonon spectrum at any lattice parameters by interpolation. The equilibrium lattice constants at temperature  $T$  is obtained by minimizing  $F$  with respect to  $a$  and  $c$ . The coefficients of linear expansion (CTE) are given by

$$\alpha_a = \frac{1}{a_{293}} \left( \frac{da(T)}{dT} \right),$$

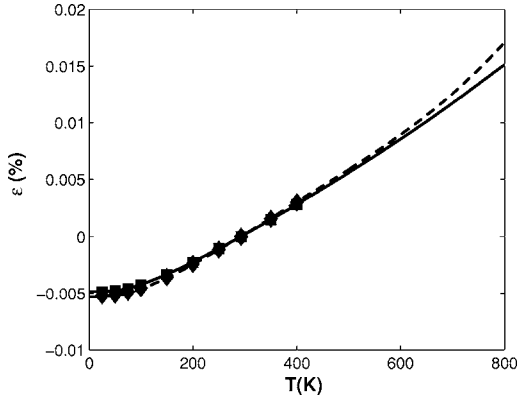


FIG. 1. Temperature dependence of the linear thermal expansion for Mg. Solid and dashed curves are the calculated result in directions perpendicular and parallel to the principal axis, respectively. Squares and diamonds represent corresponding experimental data from Ref. 19.

$$\alpha_c = \frac{1}{c_{293}} \left( \frac{dc(T)}{dT} \right), \quad (4)$$

and the thermal expansion are described by

$$\begin{aligned} \varepsilon_a &= \frac{a - a_{293}}{a_{293}}, \\ \varepsilon_c &= \frac{c - c_{293}}{c_{293}}. \end{aligned} \quad (5)$$

Here  $a$  and  $c$  mean equilibrium lattice constants at corresponding temperatures. The subscript 293 means 293 K. We have similar definitions for the coefficients of volume expansion and volume expansion.

Once phonon spectrum is obtained, we can easily calculate the vibrational heat capacity at constant volume from the next equation:

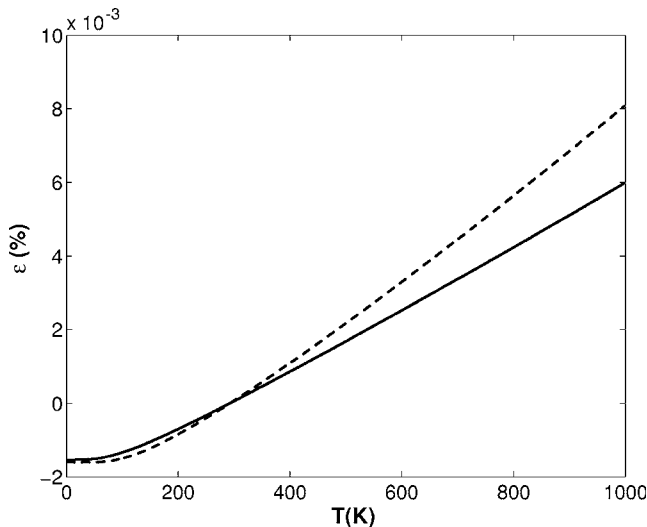


FIG. 2. Same as Fig. 1 but for Ti.

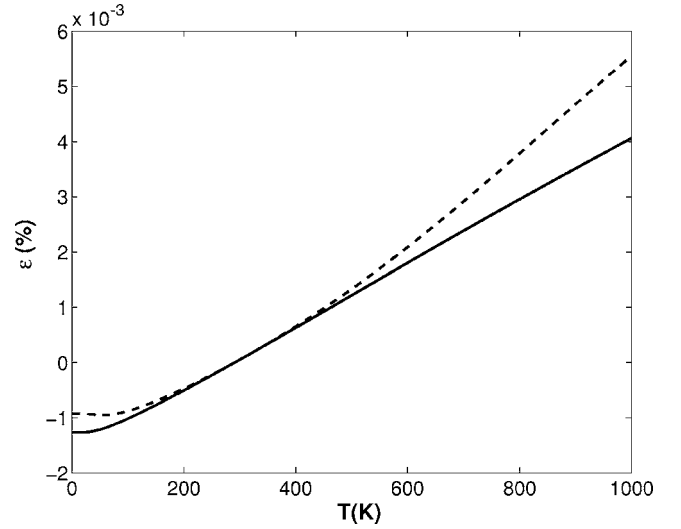


FIG. 3. Same as Fig. 1 but for Zr.

$$C_V^{\text{ph}} = k_B \sum_{q\lambda} \left( \frac{\hbar \omega_{q\lambda}(\mathbf{a})}{2k_B T} \right)^2 \text{csch}^2 \left( \frac{\hbar \omega_{q\lambda}(\mathbf{a})}{2k_B T} \right). \quad (6)$$

The electronic heat capacity can be obtained from

$$C_V^{\text{el}} = T \left. \frac{\partial S_{\text{el}}}{\partial T} \right|_V. \quad (7)$$

The heat capacity at constant pressure can be computed by using the relation

$$C_p = C_V + \alpha^2 B V T, \quad (8)$$

where  $B$  is bulk modulus,  $C_V = C_V^{\text{ph}} + C_V^{\text{el}}$ , and  $\alpha$  is coefficient of volume expansion. For hcp structure,  $\alpha = 2\alpha_a + \alpha_c$ .

### III. COMPUTATIONAL DETAILS

The thermal properties calculations of hcp metals, Mg, Ti, and Zr, were performed using the ABINIT codes.<sup>17</sup> The static energies were computed using DFT, and phonon frequencies

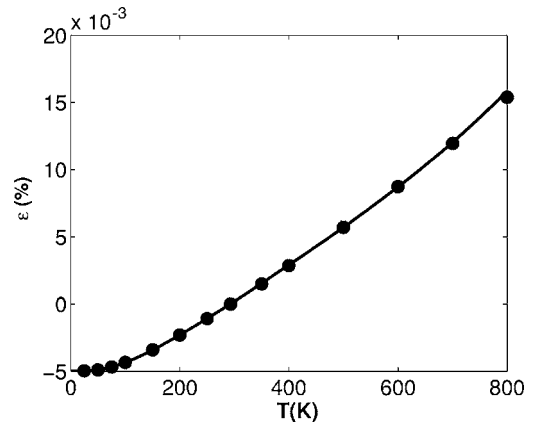


FIG. 4. Temperature dependence of the volume thermal expansion for Mg. The solid curve is the calculated result and circles represent experimental data from Ref. 19.

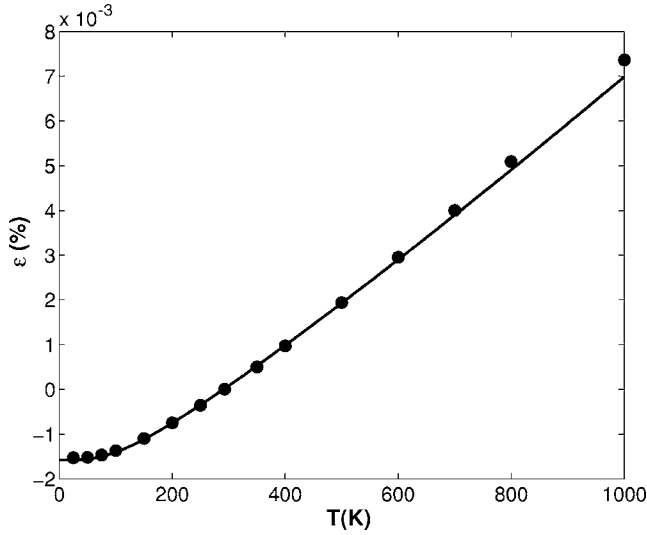


FIG. 5. Same as Fig. 4 but for Ti.

using DFPT. The interactions between the ions and valence electrons were described using norm-conserving local density approximation pseudopotentials which are generated in the scheme of Troullier–Martins.<sup>18</sup> Brillouin-zone integrations were performed using  $12 \times 12 \times 8$   $k$ -point mesh, and phonon frequencies were computed on a  $6 \times 6 \times 4$   $q$ -point mesh. Plane-wave basis sets with a cutoff of 16, 40, and 20 Hartree were used for Mg, Ti, and Zr, respectively. These calculating parameters are chosen to guarantee the total energy error in 0.1 mHartree.

To obtain the free energy, we perform 81 sets of first-principles electronic total energy and response-function calculations of Mg, Ti, and Zr by varying lattice constants  $a/a_0$  and  $c/c_0$  from 0.99 to 1.03 with a step of 0.005, respectively. At each set of  $a$  and  $c$ , the electronic free energies and entropies at several temperatures from 0 to 1000 K (for Mg, from 0 to 800 K) are obtained from the self-consistent DFT calculations using FD smearing. Then the electronic free energies and entropies at any temperature can be obtained by

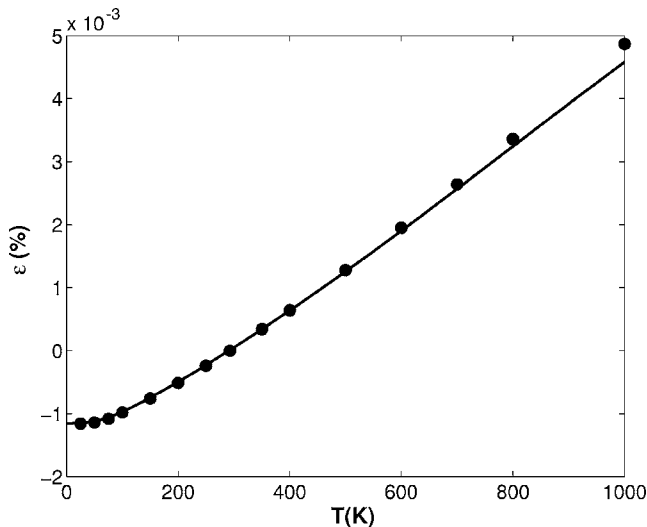


FIG. 6. Same as Fig. 4 but for Zr.

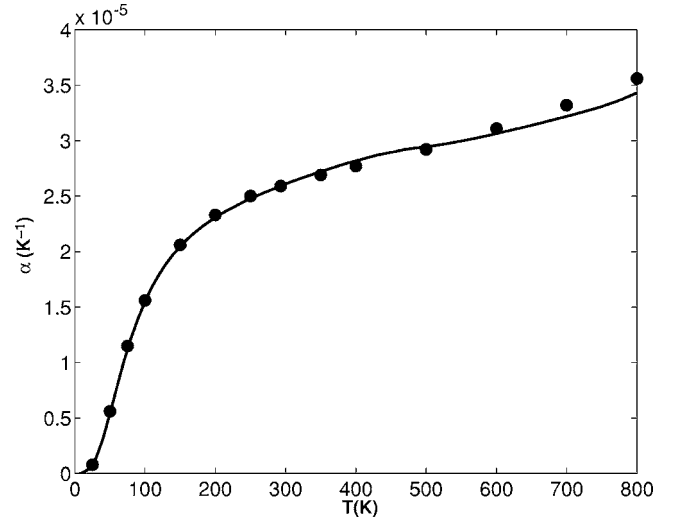


FIG. 7. Temperature dependence of the volume coefficients of thermal expansion for Mg. The solid curve is the calculated result and circles represent experimental data from Ref. 19.

interpolation. The full phonon spectrum is obtained by the Fourier interpolation algorithm of dynamical matrices. From the full phonon spectrum, the lattice vibration free energy and then the total Helmholtz free energy are calculated. In order to get the temperature dependence of lattice parameters, we calculated 81 sets of total free energy at temperature points with a step of 1 K from 0 to 1000 K (for Mg from 0 to 800 K). At each temperature point, we first fit the 81 sets free energy vs  $a$  and  $c$  with spline function and calculate the equilibrium  $a_0$  and  $c_0$  by minimizing vibration free energy. Next, fit  $a_0$  and  $c_0$  vs temperature data with spline function, respectively. This gives us the temperature dependencies of lattice parameters  $a$  and  $c$ .

## IV. RESULTS

### A. Thermal expansion

Figures 1–3 show the temperature dependence of lattice parameters  $a$  and  $c$ .

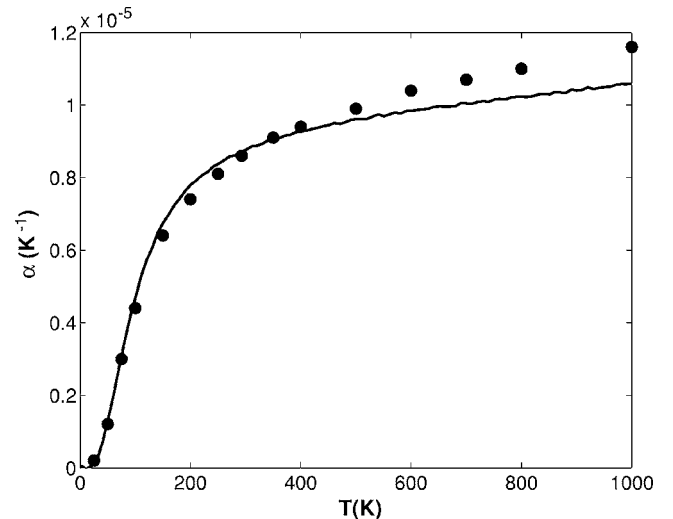


FIG. 8. Same as Fig. 7 but for Ti.

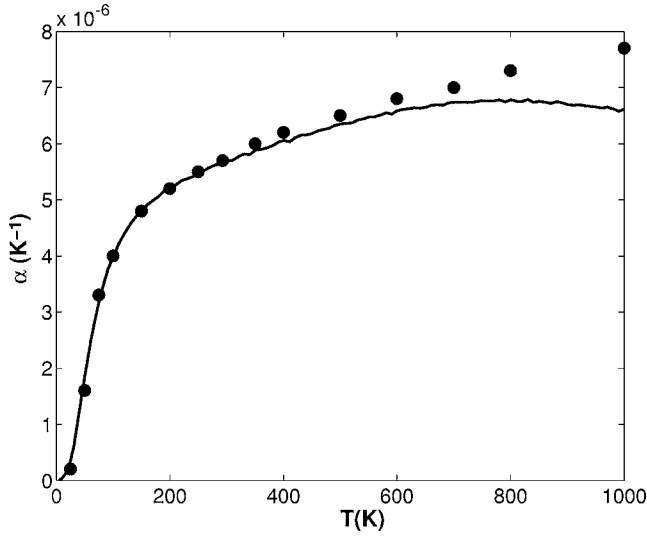


FIG. 9. Same as Fig. 7 but for Zr.

For Mg, we find excellent agreement between the theoretical results and available experimental data. For Ti and Zr, we could not find available experimental data for linear expansion. To check the theoretical results, we calculated the volume expansion from linear expansion. Figures 4–6 show the results.

They are all in good agreement with available experimental data in a wide range of temperatures, especially the results for Mg. It suggests the calculated linear expansion results for Ti and Zr are credible, although there are no available corresponding experimental data for them. Comparing the calculated and experimental values at 800 K, the calculated values are lower than the corresponding experimental values by 4% and 5% for Ti and Zr, respectively. For Mg, this relative error is only 0.5% at 800 K.

We also calculated coefficients of volume thermal expansion, as shown in Figs. 7–9. The results for Mg are in good agreement with available experimental data. At 800 K, the

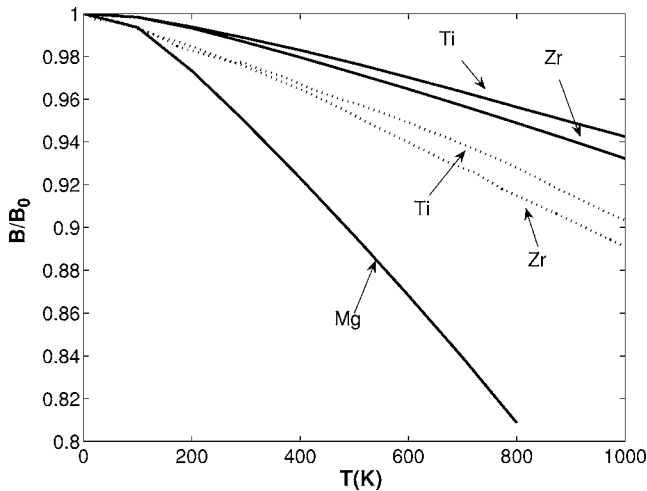


FIG. 10. Temperature dependence of the ratio of bulk modulus for Mg, Ti, and Zr. Solid and dashed curves are the calculated and experimental (Ref. 20) results, respectively.

TABLE I. Ground properties for Mg, Ti, and Zr. The experimental bulk modulus for Ti and Zr are from Ref. 20 (calculated from elastic constants at 4 K). All other experimental data are from Ref. 19.

	$a$ (Å)		$c$ (Å)		$B$ (GPa)	
	Calc.	Expt.	Calc.	Expt.	Calc.	Expt.
Mg	3.138	3.209	5.107	5.211	36.7	35.6
Ti	2.900	2.951	4.671	4.679	123	110
Zr	3.229	3.232	5.166	5.147	101	97.5

relative error is about 3%. For Ti and Zr, the errors are about 7% and they increase with temperature remarkably. These relative errors for Ti and Zr at 1000 K are about 9% and 15%, respectively.

### B. Elastic constants

The lattice constants and bulk modulus obtained for zero temperature are listed in Table I.

In all cases the calculated lattice constants are 1~2% underestimated except the  $c$  value for Zr. The bulk modulus are 3~4% overestimated for Mg and Zr, 12% for Ti.

Theoretical elastic constants calculated at 0 K are presented in Table II. The experimental values from Ref. 20 are measured at 4 K. Most calculated values and corresponding experimental data differ from each other by 10%~20%. The  $C_{44}$  for Zr has a relative error of 28%. The largest error is 61% of  $C_{66}$  for Ti.

According to linear expansion, we can obtain equilibrium lattice constants at any temperature, then the bulk modulus at any temperature can be obtained. Figure 10 shows the ratio of bulk modulus for Mg, Ti, and Zr. Comparing to experimental data, our calculated values for Ti and Zr decrease with temperature slowly. At 1000 K, they are overestimated by about 4%. For Mg, not only is the bulk modulus the smallest in these three metals, but also the cal-

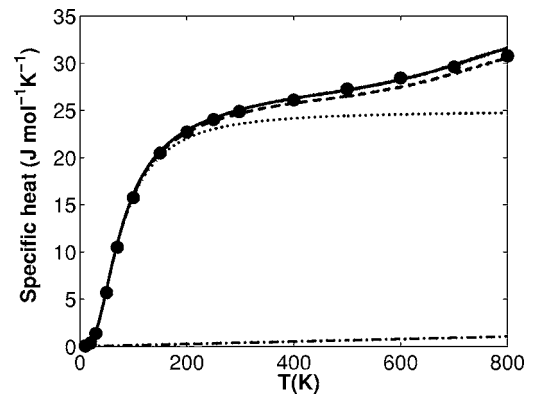


FIG. 11. Temperature dependence of heat capacity for Mg. Solid and thick dashed curves show the calculated  $C_p$ , including electronic contribution and not, respectively. Thin dashed and dot-dashed lines show vibrational and electronic  $C_v$ , respectively. Circles represent experimental data for  $C_p$ .

TABLE II. Experimental and calculated elastic constants (GPa) for Mg, Ti, and Zr, here  $C_{66} = \frac{1}{2}(C_{11} - C_{12})$ .

	Work	$C_{11}$	$C_{12}$	$C_{13}$	$C_{33}$	$C_{44}$	$C_{66}$
Mg	Calc.	65.1	23.9	21.7	65.0	17.7	20.6
	Expt. <sup>a</sup>	59.7	26.2	21.7	61.7	16.4	16.8
Ti	Calc.	219	76.6	72.8	227	50.4	71.2
	Expt. <sup>b</sup>	176	86.9	68.3	191	50.8	44.6
Zr	Calc.	155	69.1	74.7	163	26.2	43.0
	Expt. <sup>b</sup>	155	67.2	64.6	175	36.3	44.1

<sup>a</sup>Reference 19.

<sup>b</sup>Reference 20.

culated ratio decreases more rapidly with temperature raising than that for Ti and Zr. This is consistent with the fact that Mg has larger thermal expansion than Ti and Zr.

### C. Specific heat

Once the phonon spectrum over the entire Brillouin zone is available, the vibrational heat capacity at constant volume  $C_V^{\text{ph}}$  and the electronic contribution to heat capacity at constant volume  $C_V^{\text{el}}$  can be calculated by Eqs. (6) and (7), respectively. Then, the specific heat at constant pressure can be computed by Eq. (8). As a comparison, both  $C_p$  values, including electronic contribution and not, are plotted. The results are shown in Figs. 11–13. All the experimental specific heat data below are from Ref. 21.

As temperature increases,  $C_V^{\text{ph}}$  tends to the classical constant  $3R$ ;  $C_V^{\text{el}}$  and  $C_p$  still increase. We find  $C_V^{\text{el}}$  is not negligible at high temperature, though smaller than  $C_V^{\text{ph}}$ . From Figs. 11–13, once again we find good agreement between the calculated results and the experimental data for Mg, and some larger errors for Ti and Zr.

At very low temperature,  $C_V^{\text{el}}$  becomes larger than  $C_V^{\text{ph}}$ , and the discrepancy between  $C_p$  and  $C_V$  can be neglected. Figures 14–16 show the results.

The calculated values are in excellent agreement with the experimental data.

## V. DISCUSSION

Comparing with thermal expansion,  $\varepsilon$ , the errors in  $\alpha$  are larger. This is due to the numerical derivative of  $a$  and  $c$  with respect to temperature. The numerical derivative is sensitive to the errors in source data. On the other hand, the change of lattice parameters is proportional to the product of the  $\alpha$  and the change of temperature. Considering  $\varepsilon$  and  $\alpha$  have the order of magnitude  $10^{-3}$  and  $10^{-6}$ , respectively, we can expect a large relative error in  $\alpha$  causes only a small relative error in  $\varepsilon$  when the change of temperature is not large.

At high temperature, the larger errors for Ti and Zr may suggest the limitation of the quasiharmonic approximation, because the quasiharmonic approximation accounts only partially for the anharmonic effects. There should be larger anharmonic effects when the temperature rises up to  $hcp \rightarrow bcc$  phase transformation point. In quasiharmonic approximation, the phonon frequencies at given lattice parameters are independent of temperature. In real crystal, it is not the case. Anharmonic effects make each phonon frequency suffers a shift.<sup>22</sup> At high temperature, these shifts are proportional to temperature and depend on frequencies. According

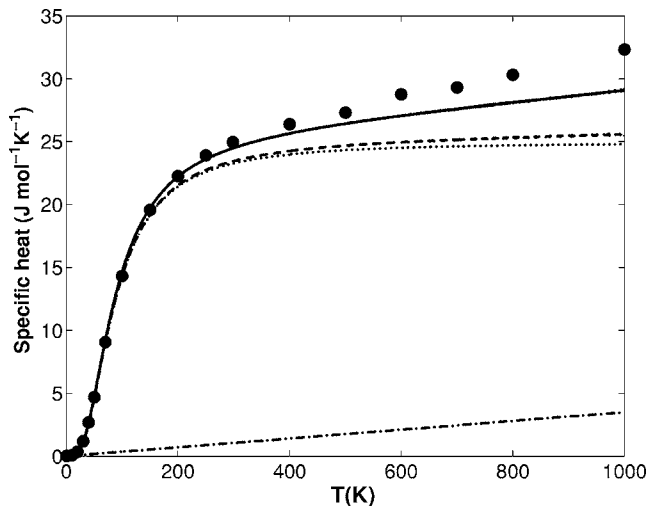


FIG. 12. Same as Fig. 11 but for Ti.

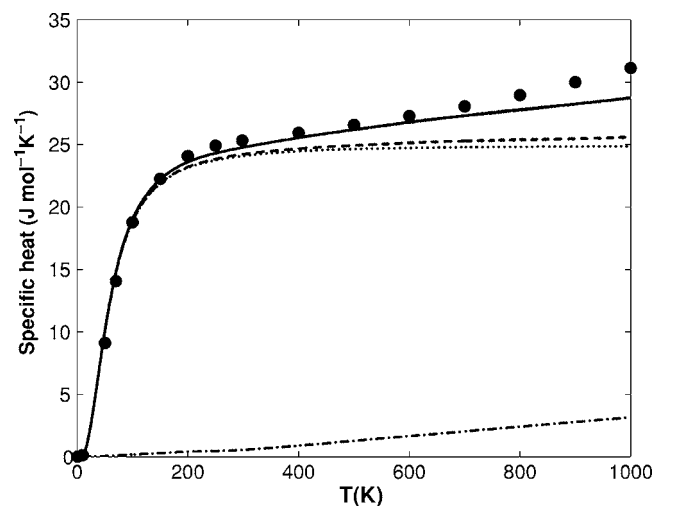


FIG. 13. Same as Fig. 11 but for Zr.

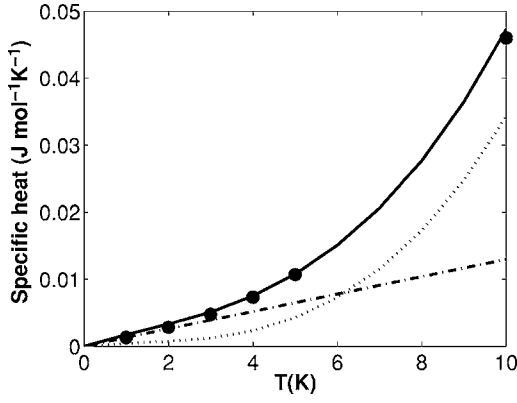


FIG. 14. Temperature dependence of heat capacity for Mg. Solid line shows the calculated  $C_p$ . Dashed and dot-dashed lines show vibrational and electronic  $C_v$ , respectively. Circles represent experimental data for  $C_p$ .

to Grüneisen relation  $\alpha = \gamma C_v / VB$ , and Grüneisen parameter  $\gamma = -d \ln \omega / d \ln V$ , we can roughly estimate that the discrepancy between  $\gamma$  calculated within quasiharmonic approximation and that, including anharmonic effects, is proportional to temperature, and then the discrepancy between calculate  $\alpha$  and the experimental data is also proportional to temperature. Another cause<sup>12</sup> of large errors at high temperature is that the LDA underestimates lattice parameters and overestimates bulk modulus, then underestimates thermal expansion. Thus, as the temperature is increased, these two effects (underestimation of lattice parameters and overestimation of bulk modulus) are both aggravated further, resulting in increasing errors.

From the results of heat capacity, the discrepancy between the calculated and experimental  $C_p$  is large for Ti and Zr, when the electronic contribution is not included. At first sight, the discrepancy may seem to be attributed to the error in  $\alpha$ . However, the error due to the underestimation of  $\alpha$  is canceled out to some extent by the overestimation of bulk modulus, when we calculate the difference  $C_p - C_v = \alpha^2 BVT$ . To check this, we calculated  $\alpha^2 BVT$ , using the experimental data for  $\alpha$ ,  $B$ , and  $V$ . It is almost the same as the theoretical

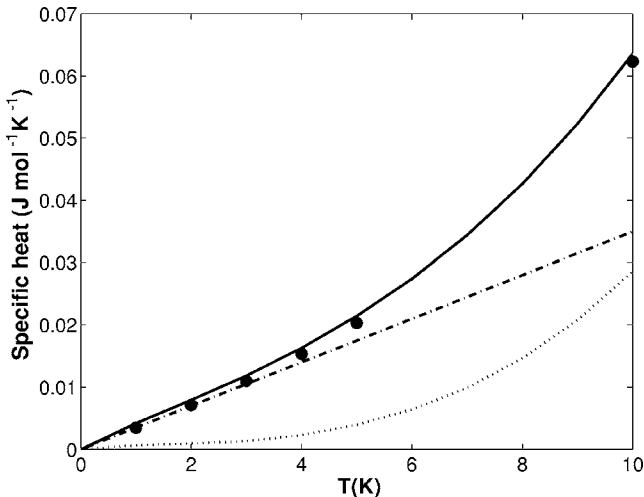


FIG. 15. Same as Fig. 14 but for Ti.

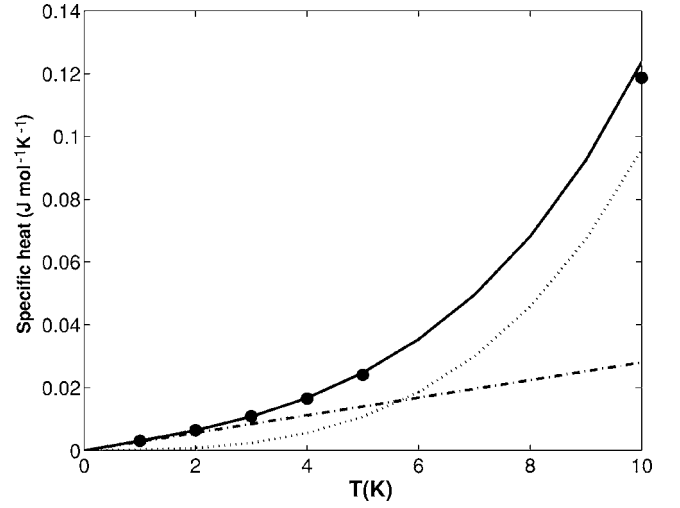


FIG. 16. Same as Fig. 14 but for Zr.

result. When we consider the electronic contribution, the theoretical  $C_p$  are improved remarkably. It is clear that the electronic contribution should be considered, especially for transition metals. Although  $C_v^{\text{el}}$  is smaller than  $C_v^{\text{ph}}$ , it is larger than the value  $C_p - C_v = \alpha^2 BVT$  for Ti and Zr. The electronic heat capacity can be expressed as  $C_v^{\text{el}} = \gamma T$ , where  $\gamma$  is known as the electronic constants. From our calculations, the values of  $\gamma$  for Mg change from (in unit  $\text{mJ mole}^{-1} \text{K}^{-2}$ ) 1.1 to 1.4 in the considering range of temperatures. For Ti and Zr, the values change from 3.2 to 3.5 and 2.8 to 3.2, respectively. As we expected, the transition metals have large  $\gamma$ , because they often have large density of states near Fermi energy. Our calculated values of  $\gamma$  are in good agreement with experimental data<sup>21</sup> at low temperature, 1.3, 3.5, and 2.8 for Mg, Ti, and Zr, respectively. However, there still remains discrepancies between the theoretical and experimental values of  $C_p$  at high temperature for Ti and Zr. At 1000 K, the discrepancies are 10% and 9.0% for Ti and Zr, respectively. The errors may arise from theory about electronic calculations at high temperature, or other nonvibrational contribution to heat capacity. Earlier calculation<sup>15</sup> of specific heat for cubic metal tungsten underestimated  $C_p$  and attributed the large discrepancy at high temperature to the failure of quasiharmonic approximation because of the large underestimation of  $\alpha$  for tungsten. In fact, we calculated the electronic contribution to the specific heat for tungsten and found good agreement between the calculated  $C_p$  and experimental data.

On the contrary, the electronic contribution to thermal expansion can be negligible in our calculations for these three metals. As an estimation, the CTE can be expressed as  $\alpha = (\gamma_{\text{el}} C_v^{\text{el}} + \gamma_{\text{ph}} C_v^{\text{ph}}) / VB$ , where  $\gamma_{\text{el}}$  and  $\gamma_{\text{ph}}$  are overall Grüneisen parameters due to electronic and vibrational contribution, respectively.  $C_v^{\text{el}}$  and  $C_v^{\text{ph}}$  are electronic and vibrational contribution to specific heat. The overall Grüneisen parameters can be calculated from  $\gamma_a$  and  $\gamma_c$ , where both electronic and vibrational  $\gamma_a$  and  $\gamma_c$  are formulated as<sup>23</sup>

$$\gamma_a = \frac{1}{2} \frac{(\partial S / \partial \ln a)_{T,c}}{C_v},$$



$$\gamma_c = \frac{(\partial S / \partial \ln c)_{T,a}}{C_V}, \quad (9)$$

where  $S$  represents electronic (vibrational) entropy and the relations give the corresponding electronic (vibrational) Grüneisen parameters. We calculated Grüneisen parameters for these three metals. For Mg, Ti, and Zr, the values of  $\gamma_{el}$  are about 2%, 10%, and 9% of  $\gamma_{ph}$ , respectively. While the values of  $C_V^{el}$  are about 2%, 7%, and 6% of  $C_V^{ph}$  at high temperature, respectively. Thus, the values of  $\alpha$  due to electronic contribution are about 0.04%, 0.7%, and 0.5% of vibrational contribution at high temperature.

According to Eq. (9), the Grüneisen parameters are functions of temperature. To check the anisotropic thermal expansion, we calculate the mean values.  $\gamma_a$  and  $\gamma_c$  for Mg are 1.67 and 1.69. The same parameters for Ti are 1.38 and 1.54, for Zr, 1.32 and 1.49. According to relations<sup>23</sup>

$$\alpha_a = \frac{C_V}{V} [(S_{11} + S_{12})\gamma_a + S_{13}\gamma_c],$$

$$\alpha_c = \frac{C_V}{V} [2S_{13}\gamma_a + S_{33}\gamma_c]. \quad (10)$$

The anisotropic thermal expansion is due to anisotropy in anharmonicity of vibrations which represented by  $\gamma_a$  and  $\gamma_c$ , and the anisotropy in the elasticity, which can be described by the ratio  $(S_{13}+S_{33})/(S_{11}+S_{12})$ . Mg has almost isotropic Grüneisen parameters, and the ratio  $(S_{13}+S_{33})/(S_{11}+S_{12}) = 1.04$ , is close to 1. Unlike the nearly isotropic thermal expansion of Mg, the theoretical thermal expansion for Ti and

Zr are anisotropic between the directions parallel and perpendicular to the principal axis. The ratios  $(S_{13}+S_{33})/(S_{11}+S_{12})$  for them are 0.98 and 0.92. According to anisotropy in elasticity, Ti and Zr should have larger expansion in  $a$  direction. However, Ti has  $\gamma_c > \gamma_a$  and the anisotropy in elasticity is small (0.98), so it shows larger expansion in  $c$  direction. For Zr, it also shows larger expansion in  $c$  direction at high temperature because of  $\gamma_c > \gamma_a$ . At low temperature, the Grüneisen parameters are smaller than the mean values, the anisotropy in elasticity (0.92) results in the larger expansion in  $a$  direction.

## VI. CONCLUSIONS

In conclusion, thermal properties of hcp metal Mg, Ti, and Zr, such as the thermal expansions and heat capacities at constant volume (pressure) are studied by DFT and DFPT calculations. The electronic contribution to heat capacity cannot be neglected, especially for transition metals, while its contribution to thermal expansion is negligible. The anisotropic thermal expansion of Ti and Zr are due to their anisotropic Grüneisen parameters, while Mg has almost isotropic thermal expansion because of its isotropic Grüneisen parameters and elasticity. The calculated results are in good agreement with available experimental data in a wide range of temperature. It suggests the anisotropic thermal expansion and other thermal properties of noncubic metals can be well calculated from this first-principles approach.

## ACKNOWLEDGMENTS

We wish to acknowledge the support of the National Natural Science Foundation of China Grant No. 50271085.

<sup>1</sup>W. Kohn and L. J. Sham, Phys. Rev. **140**, A1133 (1965).

<sup>2</sup>R. O. Jones and O. Gunnarsson, Rev. Mod. Phys. **61**, 689 (1989).

<sup>3</sup>P. Hohenberg and W. Kohn, Phys. Rev. **136**, B864 (1964).

<sup>4</sup>S. Baroni, S. de Gironcoli, A. Dal Corso, and P. Giannozzi, Rev. Mod. Phys. **73**, 515 (2001).

<sup>5</sup>V. L. Moruzzi, J. F. Janak, and K. Schwarz, Phys. Rev. B **37**, 790 (1988).

<sup>6</sup>H. M. Jin and P. Wu, J. Alloys Compd. **343**, 71 (2002).

<sup>7</sup>X.-G. Lu, M. Selleby, and B. Sundman, Acta Mater. **53**, 2259 (2005).

<sup>8</sup>B. Mayer, H. Anton, E. Bott, M. Methfessel, J. Sticht, J. Harris, and P. C. Schmidt, Intermetallics **11**, 23 (2003).

<sup>9</sup>R. Car and M. Parrinello, Phys. Rev. Lett. **55**, 2471 (1985).

<sup>10</sup>S. Baroni, P. Giannozzi, and A. Testa, Phys. Rev. Lett. **58**, 1861 (1987).

<sup>11</sup>P. Giannozzi, S. de Gironcoli, P. Pavone, and S. Baroni, Phys. Rev. B **43**, 7231 (1991).

<sup>12</sup>S. Narasimhan and S. de Gironcoli, Phys. Rev. B **65**, 064302

(2002).

<sup>13</sup>A. A. Quong and A. Y. Liu, Phys. Rev. B **56**, 7767 (1997).

<sup>14</sup>J. Xie, S. de Gironcoli, S. Baroni, and M. Scheffler, Phys. Rev. B **59**, 965 (1999).

<sup>15</sup>A. Debernardi, M. Alouani, and H. Dreysse, Phys. Rev. B **63**, 064305 (2001).

<sup>16</sup>S. Q. Wang, Appl. Phys. Lett. **88**, 061902 (3) (2006).

<sup>17</sup>X. Gonze, J. M. Beuken, R. Caracas *et al.*, Comput. Mater. Sci. **25**, 478 (2002).

<sup>18</sup>N. Troullier and J. L. Martins, Phys. Rev. B **43**, 1993 (1991).

<sup>19</sup>D. E. Gray, *American Institute of Physics Handbook* (McGraw-Hill, New York, 1972), 3rd ed..

<sup>20</sup>E. S. Fisher and C. J. Renken, Phys. Rev. **135**, A482 (1964).

<sup>21</sup>R. Hultgren, *Selected Values of the Thermodynamic Properties of the Elements* (American Society For Metals, New York, 1973).

<sup>22</sup>A. A. Maradudin and A. E. Fein, Phys. Rev. **128**, 2589 (1962).

<sup>23</sup>G. D. Barrera, J. A. O. Bruno, T. H. K. Barron, and N. L. Allan, J. Phys. Condens. Matter **17**, R217 (2005).